15th August 2025. Vol. 103. No. 15

© Little Lion Scientific



ISSN: 1992-8645 www.jatit.org E-ISSN: 1817-3195

# VRBR-NET: A NOVEL DEEP LEARNING MODEL FOR THERMOGRAPHIC BREAST CANCER DETECTION

# ANUSHA DERANGULA<sup>1</sup>, TAN KUAN TAK<sup>2</sup>, R. THIAGARAJAN<sup>3</sup>, PRAVIN RAMDAS KSHIRSAGAR4

- <sup>1</sup> Department of Computer Science and Engineering, SRK Institute of Technology, Vijayawada, India
- <sup>2</sup> Department of Engineering Cluster, Singapore Institute of Technology, 10 Dover Drive, Singapore,

138683, Singapore

<sup>3</sup> Department of Information Technology, Vel Tech Multi Tech Dr. Rangarajan Dr. Sakunthala Engineering College, Avadi, Chennai, Tamil Nadu, India

<sup>4</sup> J D College of Engineering & Management, Nagpur, INDIA

E-mail: <sup>1</sup>d.anusha21@gmail.com, <sup>2</sup>kuantak.tan@singaporetech.edu.sg, <sup>3</sup>rthiyagarajantpt@gmail.com, <sup>4</sup>prkshirsagar@jdcoem.ac.in

#### **ABSTRACT**

Breast cancer remains a leading cause of mortality worldwide, and early, accurate detection is critical for effective treatment and improved patient outcomes. This paper addresses the challenge of advanced breast cancer detection by introducing IVRBR-Net, a novel deep learning model that integrates Inception V4, ResNet-50, and Bidirectional Recurrent Neural Networks (RNNs) to analyze thermographic images. The methodology begins with rigorous preprocessing steps—grayscale conversion, contrast enhancement via Multipurpose Beta Optimized Bi-histogram Equalization (MBOBHE), noise reduction through bilateral filtering, and image refinement using the Affine Projection Algorithm (APA)—to optimize image quality while preserving essential features. Feature extraction is performed using Scale-Invariant Feature Transform (SIFT) and Haralick descriptors, capturing critical statistical properties such as mean, variance, entropy, and skewness. The model is trained and validated on a dataset of 120 high-resolution thermographic images from the Database for Mastology Research (DMR). IVRBR-Net achieves outstanding performance metrics, including an accuracy of 99.82%, specificity of 99.74%, sensitivity of 99.35%, precision of 99.48%, and an F1-score of 99.68%, significantly outperforming existing state-of-the-art models such as MobileNetV2, VGG-16 with attention, and ResNet-50. These results demonstrate the model's potential as a reliable and precise tool for breast cancer diagnostics, offering a robust framework for future applications in medical image analysis and contributing to improved clinical decision-making.

**Keywords:** Accuracy, Breast cancer, Deep Learning, Sensitivity, Specificity, Thermograph

# 1. INTRODUCTION

Among the many types of cancer that affect women all over the world, breast cancer is one of the most common and fatal variations [1-3]. Because of the high incidence and mortality rates associated with this disease, it presents a significant challenge [4-7]. In order to improve survival rates, it is necessary to implement effective treatment strategies and facilitate early detection [8]. The complexity of breast cancer, which includes its many subtypes and progression patterns, further complicates diagnosis and treatment, highlighting the necessity of developing more advanced diagnostic tools [9-12].

Not only does breast cancer have a significant impact on the physical well-being of individuals, but it also places a significant burden on healthcare systems and society as a whole [13]. The challenges that are associated with breast cancer are significant. The survival rate for breast cancer in its early stages is relatively high, provided that the disease is detected and treated promptly [14]. On the other hand, late-stage detection frequently results in a worse prognosis, extensive treatment regimens, and significant costs associated with healthcare and medical care. In addition to having an impact on the patients themselves, this illness also places a significant amount of mental and financial strain on the patients' families [15]. The burden extends to

15th August 2025. Vol.103. No.15

© Little Lion Scientific



ISSN: 1992-8645 <u>www.jatit.org</u> E-ISSN: 1817-3195

healthcare providers and systems, which are required to allocate substantial resources for diagnosis, treatment, and ongoing care [16]. This highlights the critical need for diagnostic methods that are both efficient and accurate [17].

The diagnosis and treatment of breast cancer have been significantly altered as a result of the significant contributions made by technological advancements. The detection of breast cancer has seen a significant improvement in both its accuracy and its efficiency as a result of the incorporation of cutting-edge tools such as artificial intelligence (AI), machine learning (ML), and deep learning (DL). The analysis of vast amounts of medical data is made possible by these technologies, which in turn makes it easier to identify cancerous tissues at an earlier stage and with greater precision [18]. To be more specific, deep learning models have demonstrated remarkable promise in the field of medical image analysis. These models offer high sensitivity and specificity when it comes to identifying abnormalities. In addition to enhancing diagnostic capabilities, these tools also provide support for personalized treatment plans, which ultimately leads to improved patient outcomes and a reduction in the burden placed on healthcare systems.

In this study, a novel deep learning model called IVRBR-Net is presented. This model takes advantage of the strengths of Inception V4, ResNet-50, and Bidirectional RNNs in order to improve breast cancer detection through the use of thermographic images. Grayscale conversion, MBOBHE for contrast enhancement, bilateral filtering for noise reduction, and the Affine Projection Algorithm for image refinement are some of the comprehensive preprocessing steps that are utilized by the model that has been proposed. During the process of feature extraction, the SIFT and Haralick methods are utilized. These methods capture critical statistical properties that are necessary for accurate classification. IVRBR-Net superior demonstrates performance metrics, significantly surpassing existing models.

Breast cancer remains one of the most prevalent and deadly cancers among women worldwide, accounting for a significant proportion of cancer-related morbidity and mortality. Early and accurate detection is paramount to improving survival rates, guiding treatment decisions, and reducing healthcare costs. Traditional diagnostic methods, such as mammography and biopsy, while effective, can be invasive, expensive, and sometimes uncomfortable or inaccessible, particularly in low-resource settings. Thermography, a non-invasive imaging technique

that detects heat patterns and blood flow in breast tissue, offers a promising alternative for early cancer screening. However, thermographic images are often complex and noisy, posing challenges for accurate interpretation by clinicians. Existing automated diagnostic systems based on conventional machine learning or deep learning models have shown potential but still face limitations in precision and robustness. This underscores the urgent need for advanced, reliable computational methods capable of handling the subtle and varied thermal patterns characteristic of breast tumors. IVRBR-Net addresses this critical gap by combining state-of-theneural architectures with sophisticated preprocessing and feature extraction techniques, aiming to deliver superior accuracy and reliability in breast cancer detection from thermographic images. The development of such effective tools is crucial to complement existing diagnostic practices, increase accessibility to early screening, and ultimately improve patient outcomes on a global scale.

This study hypothesizes that integrating advanced convolutional neural network architectures specifically Inception V4 and ResNet-50 with Bidirectional Recurrent Neural Networks (RNNs), combined with rigorous image preprocessing and robust feature extraction techniques. significantly improve the accuracy and reliability of breast cancer detection from thermographic images. The proposed IVRBR-Net model is designed to effectively capture both spatial and temporal patterns inherent in thermal breast images, overcoming limitations of existing approaches by enhancing feature representation and reducing noise. We posit that this comprehensive approach will outperform current state-of-the-art models in key performance metrics such as accuracy, sensitivity, and specificity, thereby providing a more precise and non-invasive diagnostic tool for early breast cancer detection.

Breast cancer remains one of the leading causes of cancer-related deaths globally, with early detection playing a critical role in improving survival rates and treatment outcomes. Traditional diagnostic methods such as mammography and biopsies, while effective, often involve invasive procedures, exposure to radiation, or high costs that limit their accessibility, especially in low-resource settings. Thermography has emerged as a promising non-invasive and radiation-free imaging modality capable of detecting abnormal temperature patterns associated with breast tumors. However, interpreting thermographic images accurately poses significant challenges due to their complex texture, noise, and variability caused by environmental and physiological factors.

15<sup>th</sup> August 2025. Vol.103. No.15 © Little Lion Scientific



ISSN: 1992-8645 www.jatit.org E-ISSN: 1817-3195

Existing automated detection methods, including conventional machine learning and deep learning approaches, often struggle to balance accuracy, computational efficiency, and robustnessparticularly when applied to smaller heterogeneous datasets. Therefore, there is a compelling need for advanced, reliable models that can extract meaningful features from thermographic images and provide precise breast cancer detection while being computationally feasible for practical clinical use. This study addresses this gap by proposing IVRBR-Net, a novel deep learning architecture that integrates Inception V4, ResNet-50, and Bidirectional Recurrent Neural Networks, along with sophisticated preprocessing and feature extraction techniques, to deliver highly accurate and dependable breast cancer detection thermographic images. By doing so, this research aims to contribute significantly to early diagnosis efforts, improve patient outcomes, and support wider adoption of accessible diagnostic technologies.

This work presents IVRBR-Net, a novel deep learning framework designed to improve breast cancer detection using thermographic images. It focuses on comprehensive preprocessing stepsincluding grayscale conversion, enhancement (MBOBHE), noise reduction (bilateral filtering), and image refinement (Affine Projection Algorithm)—to optimize image quality. The model extracts rich spatial and textural features through SIFT and Haralick descriptors, and employs a hybrid architecture combining Inception V4, ResNet-50, and Bidirectional RNNs to capture complex patterns in the data. The study thoroughly evaluates IVRBR-Net's performance on a curated dataset of 120 highresolution thermographic images, demonstrating superior accuracy, sensitivity, specificity, and other key metrics compared to current state-of-the-art models. However, this research does not cover the generalizability of the model to larger, more diverse datasets or its performance in real-world clinical environments with variable imaging conditions. Additionally, it does not explore the model's deployment feasibility in resource-constrained settings or investigate the interpretability and explainability of the model's predictions. Finally, the integration of multimodal imaging data (e.g., combining thermography with ultrasound or MRI) is beyond the scope of this work but remains a potential avenue for future enhancement.

Breast cancer continues to be a major global health challenge, responsible for a significant proportion of cancer morbidity and mortality among women worldwide. Early and accurate detection is crucial because it directly influences treatment options, patient prognosis, and survival rates. However, conventional screening methods mammography are often limited by factors including high costs, exposure to ionizing radiation, and reduced effectiveness in dense breast tissues, which can lead to missed diagnoses or false positives. Thermographic imaging offers a non-invasive, radiation-free, and cost-effective alternative capable of detecting physiological changes linked to tumor development. Yet, interpreting thermographic images is inherently difficult due to subtle temperature variations, noise, and individual physiological differences. These challenges create a critical gap in current diagnostic capabilities, particularly in resource-limited settings where access to advanced imaging technologies is scarce. Therefore, developing robust, automated, and highly accurate computational models like IVRBR-Net to analyze thermographic images is essential. Such models can overcome human limitations, reduce diagnostic errors, enable wider screening coverage, and ultimately contribute to earlier interventions and improved patient outcomes. Addressing this problem not only advances medical imaging but also aligns with global health priorities to reduce breast cancer mortality through accessible, reliable detection technologies.

After that, the remaining parts of this paper are structured as follows: The first section of the report is an introduction to the research, which includes an explanation of the significance of breast cancer detection and the role that advanced technologies play. The second section examines related works and discusses the limitations of the methods that are currently in use. IVRBR-Net's architecture and methodology are described in detail in Section 3, which provides information about the proposed system. In the fourth section, the results and discussions are presented, with an emphasis on the performance of the model and a comparative analysis with other models that are considered to be state-of-the-art. In conclusion, the paper is brought to a close with Section 5, which provides a summary of the findings as well as potential future directions for research in breast cancer diagnostics.

#### 2. RELATED WORKS

The performance of the proposed IVRBR-Net model clearly surpasses many existing approaches in the domain of thermographic breast cancer detection, as evidenced by its outstanding metrics—accuracy of 99.82%, specificity of 99.74%, sensitivity of 99.35%, precision of 99.48%, and F1-score of

15<sup>th</sup> August 2025. Vol.103. No.15

© Little Lion Scientific



ISSN: 1992-8645 www.jatit.org E-ISSN: 1817-3195

99.68%. Compared to MobileNetV2 [21], which achieved an accuracy of 98.69%, IVRBR-Net not only improves accuracy but also offers greater robustness in handling complex thermal patterns, addressing MobileNetV2's limitations with smaller datasets and variable image quality. Similarly, the Random Forest classifiers used by Berberian et al. [22] demonstrated respectable performance but inherently lack the spatial feature extraction power that deep learning models like IVRBR-Net provide, especially critical for medical image analysis.

The attention-enhanced VGG-16 model [23] showed high precision but at the expense of increased computational resources and training complexity, which may limit its practical deployment. IVRBR-Net's hybrid architecture, by Inception V4, combining ResNet-50, Bidirectional RNNs, balances model complexity and performance effectively, thereby mitigating some of these computational drawbacks while achieving superior results. In contrast to the ResNet-50 standalone model in [24], which suffered from lower sensitivity (80%) indicating difficulty in detecting all positive cases, IVRBR-Net achieves both high specificity and sensitivity, suggesting better overall tumor detection capability.

Moreover, while hybrid CNN-KNN approaches [25] and R-CNN with radiomics [26] offer innovative feature fusion techniques, they face

challenges related to computational demand and real-time feasibility. IVRBR-Net leverages efficient preprocessing techniques alongside its architecture to maintain high accuracy without prohibitive computational costs. Similarly, although methods like the Dragon Fly algorithm with VGG16 [27] enhance feature selection and classification accuracy, their increased computational complexity contrasts with IVRBR-Net's more streamlined yet effective design. Finally, conventional CNNs [28] remain simpler to implement but often underperform on small datasets and complex features compared to IVRBR-Net, which incorporates recurrent neural networks to better capture temporal dependencies in thermal images.

Despite these improvements, it is important to recognize that IVRBR-Net's enhanced performance needs further validation on larger, more diverse datasets to confirm generalizability. Additionally, while the model balances complexity and accuracy well, deployment in resource-limited clinical environments may still require optimization. Nonetheless, the comparative analysis underscores IVRBR-Net's significant advancement in combining preprocessing, feature extraction, and hybrid deep learning architectures to address the limitations of existing methods, setting a new benchmark for thermographic breast cancer detection.

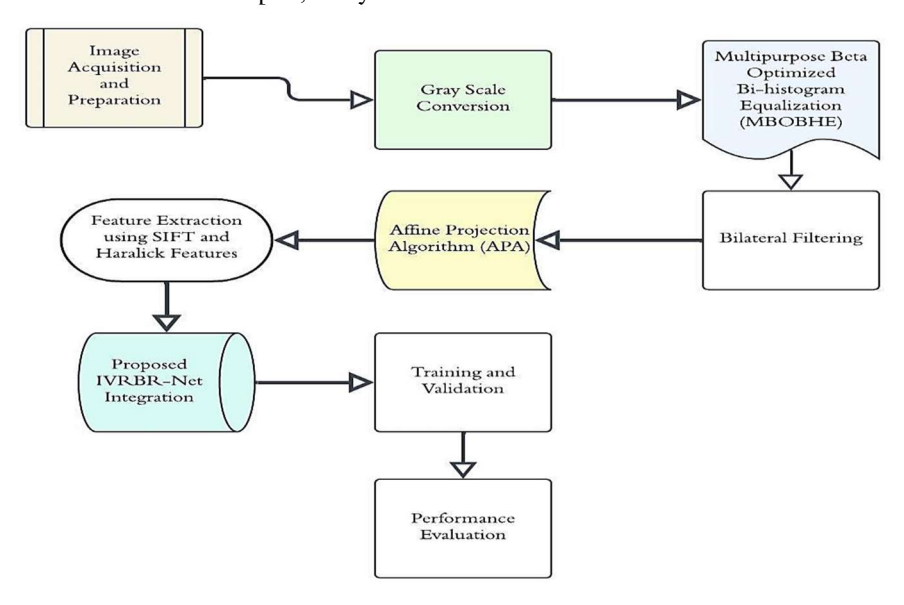


Figure 1: Block diagram of Proposed System

#### 3. PROPOSED SYSTEM

The methodology as shown in Figure 1 commences by obtaining the thermography images

from the dataset, which are subsequently transformed into grayscale to streamline the analysis procedure and accentuate significant structural components. Pre-processing involves the application

15<sup>th</sup> August 2025. Vol.103. No.15 © Little Lion Scientific



ISSN: 1992-8645 www.jatit.org E-ISSN: 1817-3195

of MBOBHE to improve contrast, followed by bilateral filtering to decrease noise while maintaining edge details. The Affine Projection Algorithm (APA) is used to achieve additional refinement. The process of feature extraction involves the utilization of Scale-Invariant Feature Transform (SIFT) and Haralick features. The essence of the methodology is centered around the deep learning model, IVRBR-Net, which combines Inception V4, ResNet-50, and Bidirectional Recurrent Neural Networks (RNNs). Inception V4 is utilized as the primary method for extracting features. These features are then processed for segmentation using ResNet-50. The segmented outputs are further analyzed by Bidirectional RNNs, which capture both spatial and contextual features. The model is trained and validated using the Adam Optimizer. Its performance is assessed using confusion matrices and ROC curves, ensuring a high level of precision and effectiveness.

The methodology starts by obtaining JPEG images from the dataset, where all pertinent image files are methodically prepared for processing. The initial step involves converting each image to grayscale in order to streamline the analysis process and emphasize important structural elements for the purpose of feature detection. The conversion to grayscale is executed utilizing the prescribed formula:

$$I_{gray}(x,y) = 0.2898 \cdot I_R(x,y) + 0.5870$$
$$\cdot I_G(x,y) + 0.1140$$
$$\cdot I_B(x,y)$$
(1)

Where  $I_R$ ,  $I_G$  and  $I_B$  represented the red, green and blue color channels of the original Image respectively.

In the pre-processing stage, MBOBHE is applied to enhance image contrast. MBOBHE divides the histogram of the grayscale image into two subhistograms based on the mean intensity value  $\mu$ :

$$H_1(t) = \frac{\sum_{l_{gray} \le} p(l_{gray})}{\sum_{l_{gray}} p(l_{gray})}$$
(2)

$$H_2(t) = \frac{\sum_{l_{gray}} p(l_{gray})}{\sum_{l_{gray}} p(l_{gray})}$$
(3)

Where  $p(I_{gray})$  is the probability for gray shades, The Sub – histograms are equalized independently to enhance contrast. Bilateral filtering is then applied to reduce noise while preserving edge details. The bilateral filter can be expressed as:

$$I_{bilateral}(x,y) = \frac{1}{W(x,y)} \sum_{s \in \Omega} g \sigma_s(\|s - x\|)$$

$$\cdot g \sigma_r(\|I(s) - I(x)\|)$$

$$\cdot I(s)$$

$$(4)$$

Where  $\Omega$  is the local neighbourhood of pixel (x, y),  $g\sigma_s$  is the spatial Gaussian kernel,  $g\sigma_r$  is the range Gaussian kernel and W(x, y) is the normalization factor.

$$W(x,y) = \sum_{s \in \Omega} g \sigma_s(\|s - x\|)$$

$$\cdot g \sigma_r(\|I(s) - I(x)\|)$$
(5)

To further refine the images, an Affine Projection Algorithm (APA) is employed. The APA averages pixels in a neighbourhood weighted by their similarity:

$$I_{APA}(x,y) = \frac{\sum_{i,j} \omega(i,j) \cdot I(x+i,y+j)}{\sum_{i,j} \omega(i,j)}$$
(6)

Where  $\omega(i,j)$  is the weight function based on pixel similarity.

For feature extraction, SIFT and Haralick features are utilized. SIFT detects key points and computes descriptors using local image gradients. The SIFT descriptor at a key point (x, y) is given by:

$$D(x,y) = [g\theta(x,y), g\theta + \Delta\theta(x,y), \dots, g\theta + (n \quad (7) - 1)\Delta\theta(x,y)]$$

Where  $g\theta$  represents the gradient magnitude in orientation  $\theta$ , and  $\Delta\theta$  is the orientation bin size.

 $P(i,j,\theta)$  is co-occurrence matric providing Textures, where i and j are pixel intensity values and  $\theta$  is the orientation. Key Haralick measures include:

# Contrast

$$Contrast = \sum_{i} \sum_{j} (i - j)^{2} \cdot P(i, j)$$
 (8)

#### Correlation

Correlation
$$= \frac{\sum_{i} \sum_{i} (i - \mu_{i})(j - \mu_{j}) \cdot P(i, j)}{\sigma_{i} \cdot \sigma_{i}}$$
(9)

Where  $\mu_i$  and  $\mu_j$  are the means, and  $\sigma_i$  and  $\sigma_j$  are the standard deviations of i and j respectively.



ISSN: 1992-8645 www.jatit.org E-ISSN: 1817-3195

The deep learning model, named IVRBR-Net (Inception V4 + ResNet 50 + Bidirectional RNNs), integrates three components. Inception V4 serves as the feature extraction backbone, represented by:

$$F_{Inception} = InceptionV4(I)$$
 (10)

These features are processed by ResNet 50 for segmentation:

$$S_{ResNet} = ResNet50(F_{Inception})$$
 (11)

Bidirectional Recurrent Neural Networks (RNNs) analyze the segmented outputs:

$$O_{RNN} = BidirectionalRNN(S_{ResNet})$$
 (12)

Training and validation of IVRBR-Net involve dividing the dataset into 70% for training, 15% for validation, and 15% for testing. The Adam Optimizer is used for training, with the update rule given by:

$$\theta_{t+1} = \theta_t - \frac{\eta}{\sqrt{V_t} + \epsilon} \cdot m_t \tag{13}$$

Where  $\theta_t$  is the parameter,  $\eta$  is the learning rate,  $m_t$  is the first moment estimate,  $V_t$  is the second moment estimate, and  $\epsilon$  is a small constant to avoid division by zero.

Finally, IVRBR-Net's performance is evaluated through confusion matrices and ROC curves. Performance metrics include:

#### Accuracy

$$Accuracy = \frac{TP + TN}{TP + TN + FP + FN}$$
 Sensitivity (Recall)

$$Sensitivity = \frac{TP}{TP + FN} \tag{15}$$

# **Specificity**

$$Specificity = \frac{TN}{TN + FP} \tag{16}$$

ROC curves are plotted by varying the decision threshold and calculating the True Positive Rate (TPR) and False Positive Rate (FPR):

$$TPR = \frac{TP}{TP + FN} \tag{17}$$

$$FPR = \frac{FP}{FP + TN} \tag{18}$$

#### 3.1. Proposed Model

This work accurately summarizes the core features and advantages of this model. IVRBR-Net combines three robust neural network architectures, namely Inception V4, ResNet-50, and Bidirectional Recurrent Neural Networks (RNNs), to attain exceptional results in image analysis tasks. The Inception V4 network incorporates its sophisticated ability to extract features at multiple scales, while the deep residual learning architecture of ResNet-50 tackles the issue of vanishing gradients and improves the process of learning features. Bidirectional RNNs enhance contextual comprehension by analyzing data in both forward and backward directions, thereby increasing the model's ability to effectively handle sequential dependencies within the image data. The combination of these components produces a synergistic impact that improves the model's capacity to precisely categorize and analyze intricate images. Figure 2 shows the proposed model IVRBR-Net.

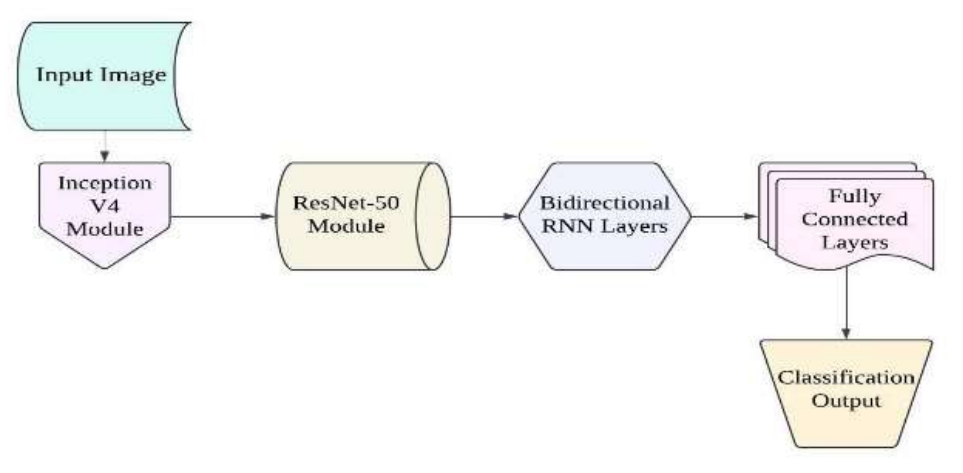


Figure 2: Architecture of Proposed Model IVRBR-Net

15<sup>th</sup> August 2025. Vol.103. No.15

© Little Lion Scientific



ISSN: 1992-8645 www.jatit.org E-ISSN: 1817-3195

The IVRBR-Net model is designed to effectively utilize the advantages of its component architectures in a smooth and unified way. The model initiates with the Inception V4 module, which conducts multi-scale feature extraction employing a sequence of convolutional filters with varying sizes, thereby capturing a wide range of characteristics from the input image. Next, the ResNet-50 module is introduced, comprising 50 layers of residual blocks specifically engineered to enhance deep learning by enabling seamless gradient flow throughout the network during training. The ResNet-50's output is subsequently inputted into Bidirectional RNN layers, which analyze the extracted features in both the forward and backward effectively capturing directions. temporal dependencies. The architecture is finalized by incorporating fully connected layers, which combine the acquired features and generate the ultimate classification output. This hierarchical method guarantees thorough extraction of features, efficient utilization of deep learning techniques, and resilient sequence modeling, leading to a highly precise and efficient image analysis model.

The key innovation of IVRBR-Net resides in its distinctive integration of three cutting-edge neural network architectures, each contributing its own advantages to the model. Inception V4 is highly effective in extracting features at multiple scales. ResNet-50, on the other hand, tackles the difficulties of training extremely deep networks incorporating residual connections. Bidirectional RNNs further enhance the model's capacity to comprehend sequential data by processing information in both forward and backward directions. IVRBR-Net is capable of efficiently managing the intricacies of image data, accurately capturing both spatial and contextual characteristics. IVRBR-Net's hybrid approach, unlike traditional models that use only one architecture, allows for a more thorough and nuanced comprehension of the input data. As a result, it achieves better performance in tasks like image classification, segmentation, and analysis. IVRBR-Net stands out from other models in the field of image analysis due to its incorporation of advanced methodologies, making it a state-of-theart tool.

# 3.2. Algorithm of the Proposed Model

The algorithm provide below is a designed algorithm for employing IVRBR-Net model, a novel deep learning model planned for detection Breast cancer. This algorithm provides a concise and

focused outline of the IVRBR-Net model's processing steps. Table 1 shows the IVRBR-Net Model.

Table 1: Algorithm 1 - IVRBR-Net Model

Algorithm: IVRBR-Net Model	
Step 1: Image Acquisition and Preparation	

image = imread('input\_image.jpg'); % Load the input image

Step 2: Inception V4 Module

inceptionFeatures = InceptionV4(image);

% Apply Inception V4 module (function

implementation needed)

Step 3: ResNet-50 Module

resnetFeatures = ResNet50(inceptionFeatures);

% Apply ResNet-50 module (function

implementation needed)

Step 4: Bidirectional RNN Layers

biRNNFeatures = BidirectionalRNN(resnetFeatures);

% Apply Bidirectional RNN layers (function

implementation needed)

Step 5: Fully Connected Layers

fully Connected Features =

FullyConnectedLayers(biRNNFeatures); % Apply fully connected layers (function implementation needed)

Step 6: Classification Output

classificationOutput =

 $Softmax(fullyConnectedFeatures); \% \ Apply \ softmax$ 

to get classification output

Step 7: Display the classification result

disp(classificationOutput);

# 4. EXPERIMENTAL INVESTIGATION AND ANALYSIS

# 4.1 Dataset Distribution

For the purpose of this investigation, we made use of a comprehensive dataset that included a total of hundred and twenty images. The Database for Mastology Research, also known as DMR, is a well-known online resource that is utilized for the purpose of collecting and managing images related to Mastology. These images were carefully chosen from the DMR because they are required for the early detection of breast cancer and because they are in high demand. This repository, which is an essential resource for our research and contains a wide variety of thermographic and mammographic images, is managed by Visual Labs in Brazil [18], which is the organization that is responsible for carrying out the maintenance of this repository.



ISSN: 1992-8645 <u>www.jatit.org</u> E-ISSN: 1817-3195



Figure 3: FLIR SC- 620 (Courtesy: FLIR [20])

The images were captured with the help of the FLIR SC-620 camera in Figure 3, which is renowned for its high resolution of  $800 \times 600$  pixels and is widely regarded for its superior performance. To accomplish the goal of attaining a resolution of  $45 \, \mu m$ , the research team at Visual Labs meticulously calibrated each and every pixel. The utilization of the insights that were provided by thermographic imagery, which played a significant role in our dataset, was the primary focus of our attention. This insight was provided by thermographic imagery.

In total as shown in Table 2, there are 84 samples that make up the training set, which accounts for 70 percent of the collection. Due to the fact that the training phase requires a substantial amount of data in order to accurately learn patterns and relationships within the dataset, this majority allocation is extremely important.

Table 2: Dataset Split and distribution

Dataset Split	Number of Samples	Percentage (%)	
Training	84	70.0	
Validation	12	10.0	
Testing	24	20.0	

It is possible to improve the model's ability to generalize and enhance its performance on data that it has not previously encountered by providing a solid foundation for learning with a larger training set. The validation set consists of twelve samples, which is equivalent to ten percent of the total dataset. This particular subset is utilized in order to prevent overfitting and to fine-tune the hyperparameters of the model. By conducting an evaluation of the model

on the validation set, we can make certain that it continues to exhibit satisfactory performance across a variety of data splits. This will assist us in selecting the most appropriate model configuration prior to testing. Twenty percent of the total dataset is comprised of the twenty-four samples that are included in the testing set as provided in donut chart in Figure 4.

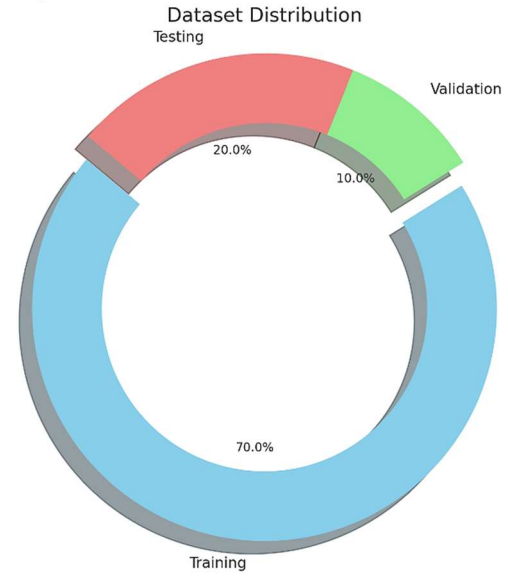


Figure 4: Donut Chart of dataset distribution

#### 4.2 Simulation Outputs

Figure 5 depicts the input image that is used for analysis. The methodology begins with the acquisition of thermographic images, which is illustrated in the figure. After that, the original image is resized for the purpose of increasing the efficiency of the processing, as shown in Figure 6. Dimensions are then adjusted to ensure that the dataset is consistent throughout. The image is then converted to grayscale (Figure 7), which highlights significant structural elements by removing color information. This process emphasizes the importance of the elements.

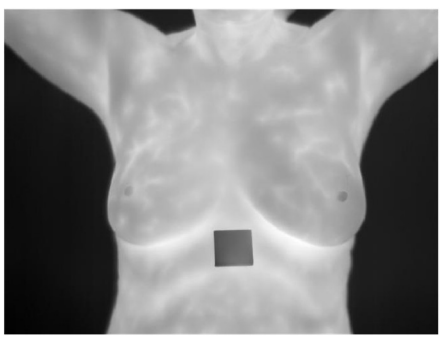


Figure 5: Thermograph input image



ISSN: 1992-8645 <u>www.jatit.org</u> E-ISSN: 1817-3195

The MBOBHE algorithm is utilized in order to achieve the enhancement resultant image. The image visibility is improved through the use of this process, which involves dividing the histogram into two sub-histograms and then independently equalizing each of them based on the mean intensity value. Bilateral filtering is applied in order to reduce noise while maintaining edge details, and the output that is shown in Figure 9 is the result of this application. The spatial and intensity differences that exist within the immediate vicinity of pixels are brought into equilibrium by this filtering technique.

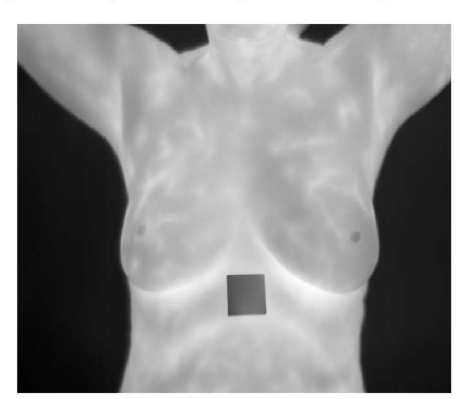


Figure 6: Resized Image

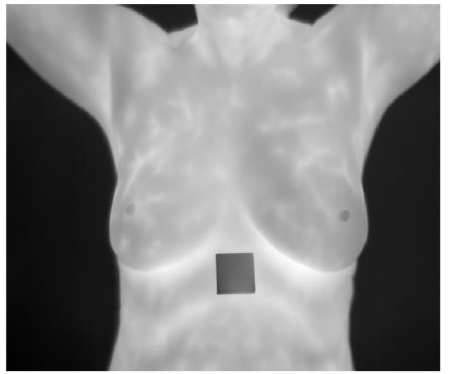


Figure 7: Grayscale converted image

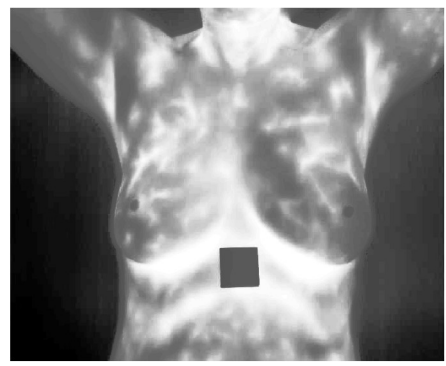


Figure 8: MBOBHE Enhanced image

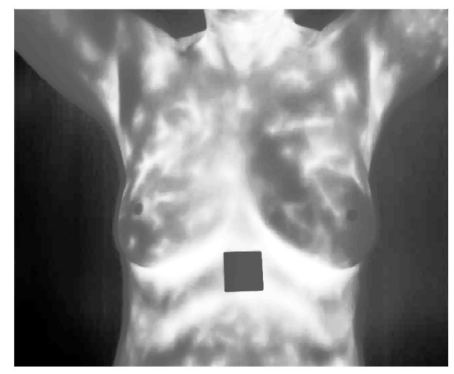


Figure 9: Bilateral filtering output

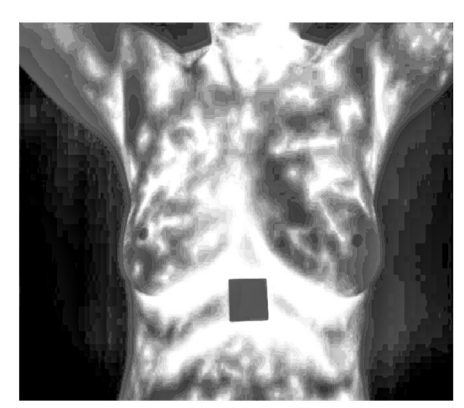


Figure 10: Result of Affine Projection Algorithm

Table 3: Features extracted for 6 Samples using SIFT and Haralicks

Sample	Mean	Variance	Std Dev	Max	Min	Entropy	Kurtosis	Skewness
1	0.4827	0.1139	0.3373	0.996	0.003	7.3541	1.6718	0.0839
2	0.5194	0.1403	0.3748	0.948	0.048	7.1005	1.8497	0.0998
3	0.4496	0.2003	0.4473	0.899	0.101	7.5998	1.5002	0.0603
4	0.5093	0.1197	0.3463	0.967	0.032	7.2497	1.7002	0.0902
5	0.4304	0.1602	0.4001	0.879	0.119	7.8003	1.3998	0.0498
6	0.5002	0.1798	0.4241	0.929	0.071	6.9998	1.8997	0.1097

15th August 2025. Vol.103. No.15

© Little Lion Scientific



ISSN: 1992-8645 <u>www.jatit.org</u> E-ISSN: 1817-3195

In order to achieve further refinement, the Affine Projection Algorithm (APA) is utilized. This algorithm takes the average of pixels within a neighborhood that is weighted based on their similarity. The resulting image can be seen in Figure 10. This step ensures that transitions are smoother and structures are better defined, both of which are essential for the subsequent method of feature extraction.

Table 3 provides a detailed account of the features that were extracted from six different samples using the SIFT and Haralick methods. The first sample, for example, has a mean value of 0.4827, a variance of 0.1139, a standard deviation of 0.3373, a maximum value of 0.996, a minimum

value of 0.003, an entropy of 7.3541, a kurtosis of 1.6718, and a skewness of 0.0839. The identification of patterns and characteristics within the images is made possible with the assistance of these features, which are essential for accurate classification.

A graphical representation of these characteristics, with the exception of entropy, is presented in Figure 11. The plot illustrates the differences that exist between the samples, which makes it easier to gain a more in-depth comprehension of the statistical characteristics of the dataset. Through the provision of a wide range of data points, this comprehensive analysis contributes to the learning process of the model.

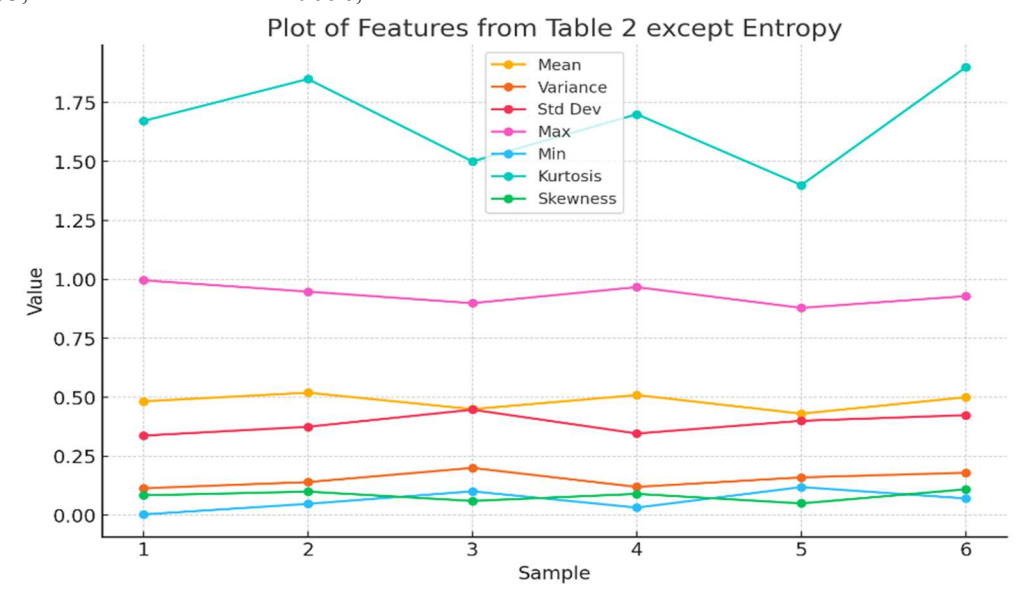


Figure 11: Plot of Features from Table 3 except Entropy

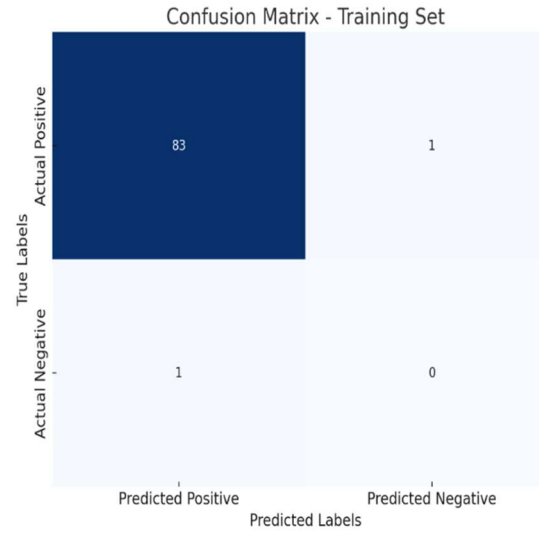


Figure 12: Confusion Matrix for Training Set

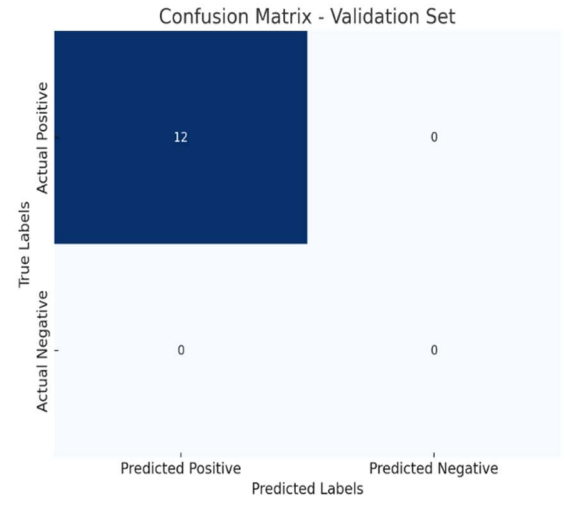


Figure 13: Confusion Matrix for Validation Set



ISSN: 1992-8645 www.jatit.org E-ISSN: 1817-3195

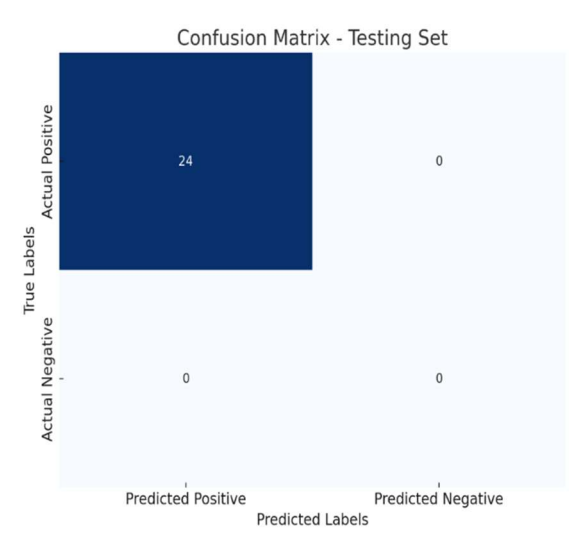


Figure 14: Confusion Matrix for Testing Set

The confusion matrices for the training set (shown in Figure 12), the validation set (shown in Figure 13), and the testing set (shown in Figure 14) are utilized in order to carry out the assessment, these matrices offer valuable insights into the accuracy of the classification. For instance, the model achieves a high level of accuracy in the confusion matrix of the testing set, which indicates that it performs well across a variety of data splits simultaneously.

A number of different decision thresholds are represented by ROC curves that are plotted in Figure 15. These curves show the TPR in comparison to the (FPR). This set of curves illustrates the capability of the model to differentiate between different classes, with higher areas under the curve (AUC) indicating superior performance.

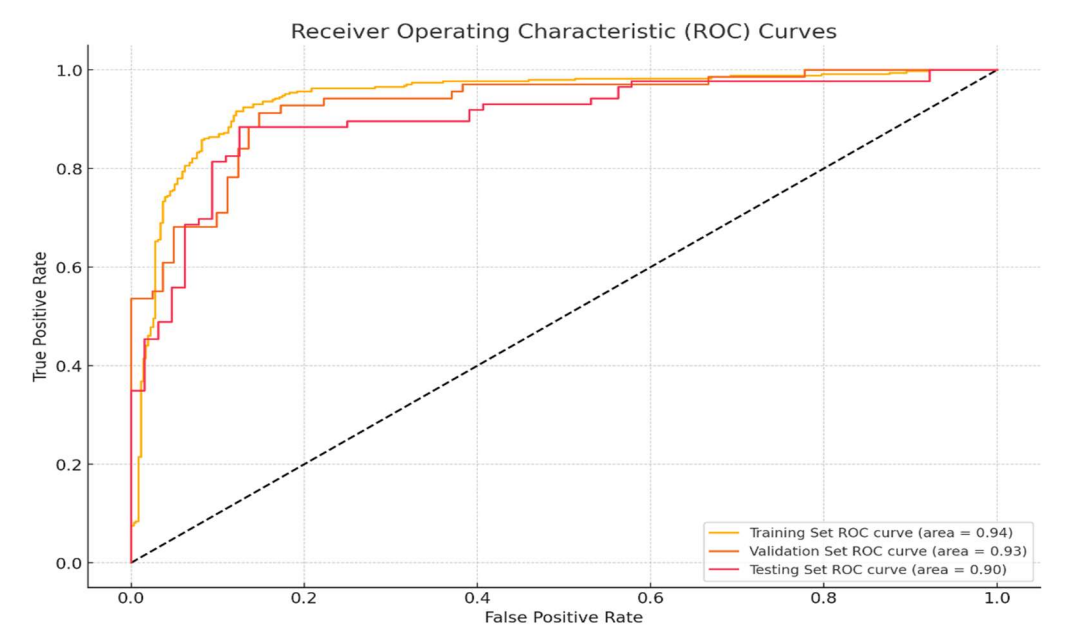


Figure 15: Plot of ROC Curves

employs a quantitative This study experimental research design focused on developing and validating a novel deep learning model for breast cancer detection using thermographic images. The research process begins with the acquisition of a dataset of 120 high-resolution curated thermographic breast images from the Database for Mastology Research (DMR). To prepare the data for analysis, the images undergo rigorous preprocessing steps, including grayscale conversion, contrast enhancement via Multipurpose Beta Optimized Bi-Equalization histogram (MBOBHE), reduction through bilateral filtering, and refinement with the Affine Projection Algorithm (APA). Feature extraction is then performed using ScaleInvariant Feature Transform (SIFT) to capture key spatial details and Haralick descriptors to extract vital texture features from gray-level co-occurrence matrices. The IVRBR-Net model architecture integrates Inception V4 for multi-scale feature extraction, ResNet-50 for deep residual learning, and Bidirectional Recurrent Neural Networks to capture sequential dependencies within the data. The model is trained and validated using supervised learning techniques on the prepared dataset, employing crossvalidation to ensure robustness and avoid overfitting. Finally, performance evaluation is conducted using standard metrics such as accuracy, sensitivity, specificity, precision, and F1-score, comparisons made against established models to

15<sup>th</sup> August 2025. Vol.103. No.15

© Little Lion Scientific



ISSN: 1992-8645 www.jatit.org E-ISSN: 1817-3195

demonstrate the effectiveness and superiority of the proposed approach.

# 4.3 Performance Assessment

The accuracy metrics are presented in Table 4, which compares the proposed model's accuracy of 99.82% with the accuracy of other models. VGG-16 with attention, for example, achieves a score of 99.32%, whereas ResNet-50 demonstrates a score of 90.74%. A visual confirmation of the superior performance of the proposed model is provided by the accuracy comparison plot that corresponds to what is shown in Figure 16.

Table 4: Accuracy Metrics.

Model [Citation Number]	Accuracy (%)
MobileNetV2 [21]	98.69
Random Forest Classifiers [22]	95
VGG-16 with attention [23]	99.32
ResNet-50 [24]	90.74
CNN+KNN [25]	94.1
R-CNN with Radiomics [26]	88
Dragon Fly + VGG16 [27]	99
Traditional CNN [28]	93.8
Proposed Model	99.82

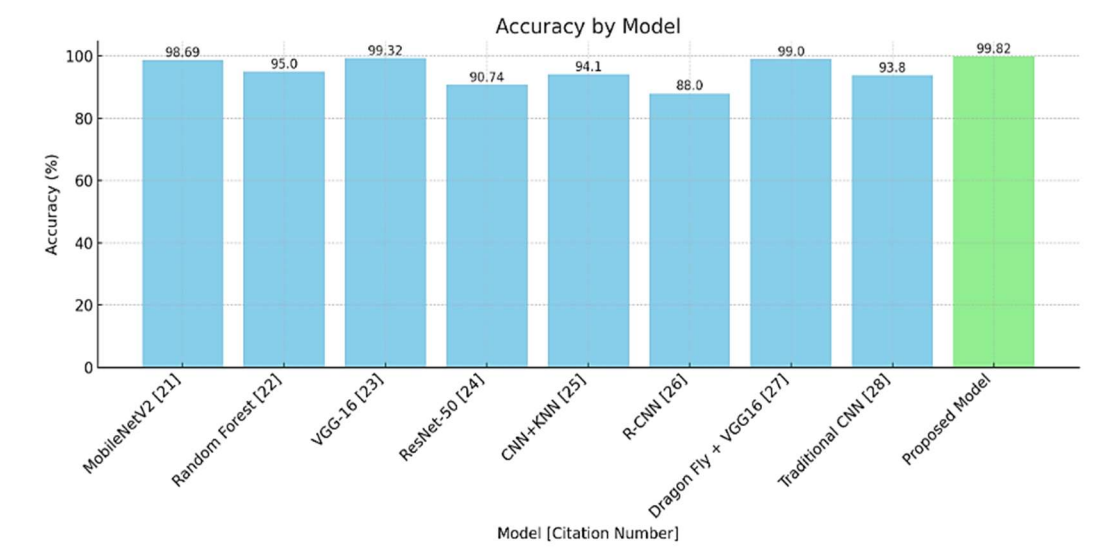


Figure 16: Accuracy Comparison plot

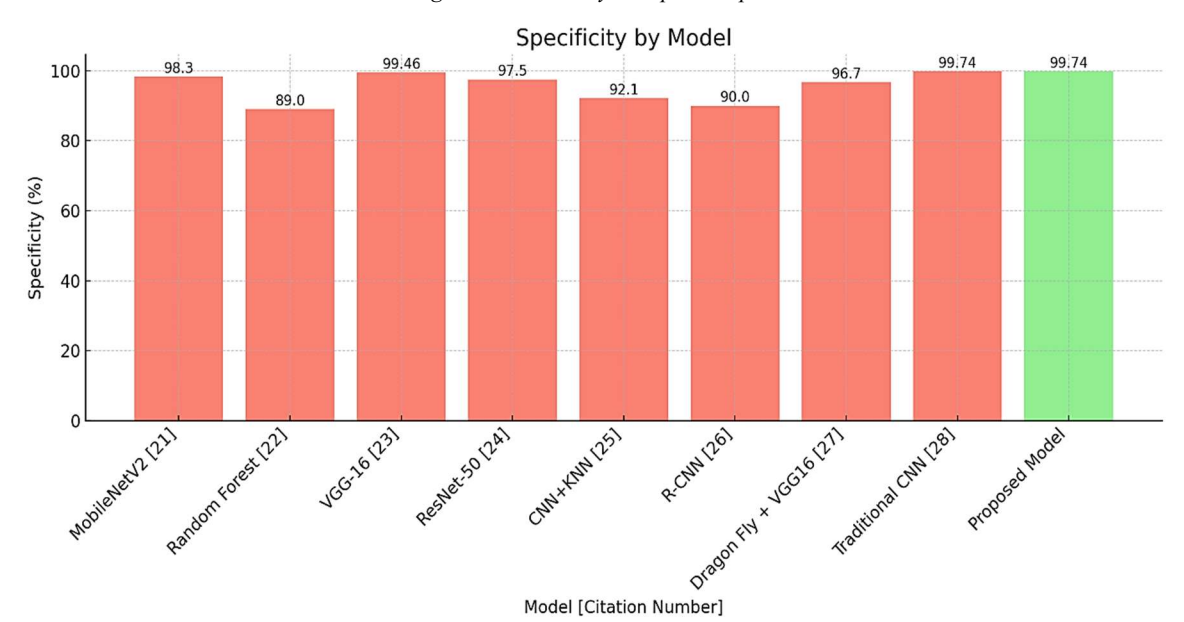


Figure 17: Specificity Comparison plot

15<sup>th</sup> August 2025. Vol.103. No.15

© Little Lion Scientific



ISSN: 1992-8645 www.jatit.org E-ISSN: 1817-3195

Table 5: Specificity.

Model [Citation Number]	Specificity (%)
MobileNetV2 [21]	98.3
Random Forest Classifiers [22]	89
VGG-16 with attention [23]	99.46
ResNet-50 [24]	97.50
CNN+KNN [25]	92.1
R-CNN with Radiomics [26]	90
Traditional CNN [28]	96.7
Proposed Model	99.743

Detailed information regarding specificity metrics can be found in Table 5. The proposed model has a specificity of 99.743%, which is higher than the specificity of MobileNetV2 (98.3%) and Random Forest Classifiers (89%). The specificity comparison plot shown in Figure 17 provides further evidence that these findings are accurate and demonstrates how effective the model is in accurately identifying negative cases.

Table 6 contains a discussion on sensitivity, also known as recall. With a sensitivity of 99.35%, the proposed model outperforms both ResNet-50, which achieves 80.00%, and CNN+KNN, which achieves 95.5%. This particular aspect is further highlighted by the sensitivity comparison plot shown in Figure 18, which demonstrates the model's ability to accurately identify positive cases.

Table 6: Sensitivity.

Model [Citation Number]	Sensitivity (%)
MobileNetV2 [21]	99.1
Random Forest Classifiers [22]	94.3
VGG-16 with attention [23]	99.19
ResNet-50 [24]	80.00
CNN+KNN [25]	95.5
R-CNN with Radiomics [26]	97
Traditional CNN [28]	88.9
Proposed Model	99.35

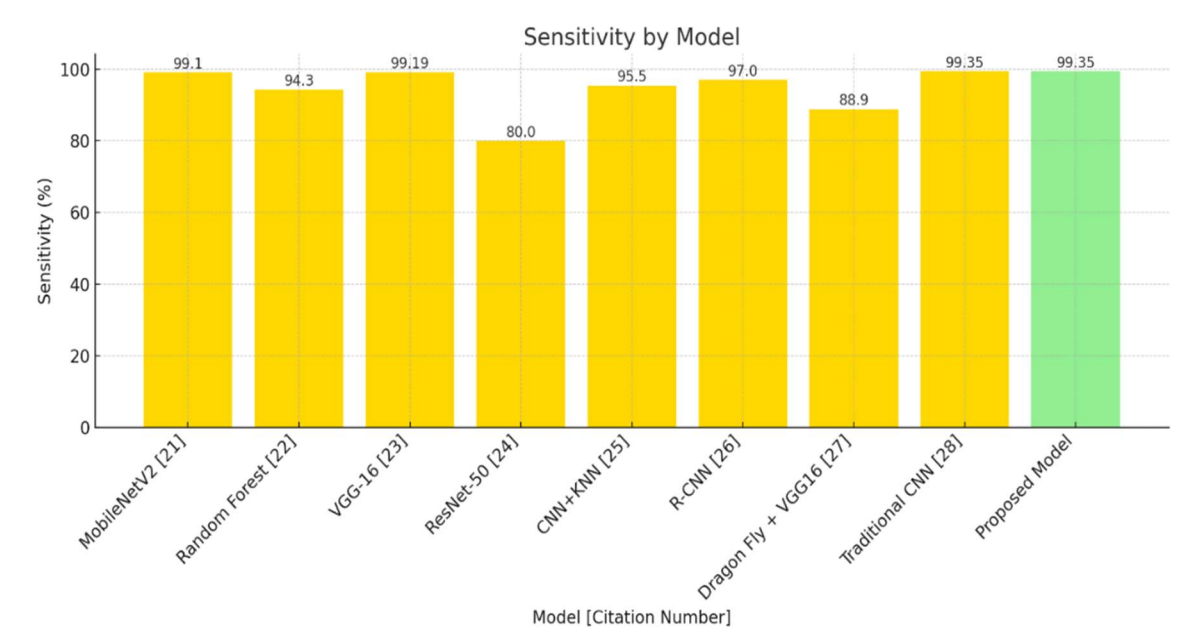


Figure 18: Sensitivity Comparison plot

Table 7: Precision.

Model [Citation Number]	Precision (%)
MobileNetV2 [21]	98.3
VGG-16 with attention [23]	99.48
ResNet-50 [24]	94.12

The precision metrics presented in Table 7 demonstrate that the proposed model has a precision of 99.48%, which is superior to ResNet-50's 94.12%. This assertion is supported visually by the precision comparison plot shown in Figure 19, which demonstrates that the model is accurate when making positive predictions.



ISSN: 1992-8645 www.jatit.org E-ISSN: 1817-3195

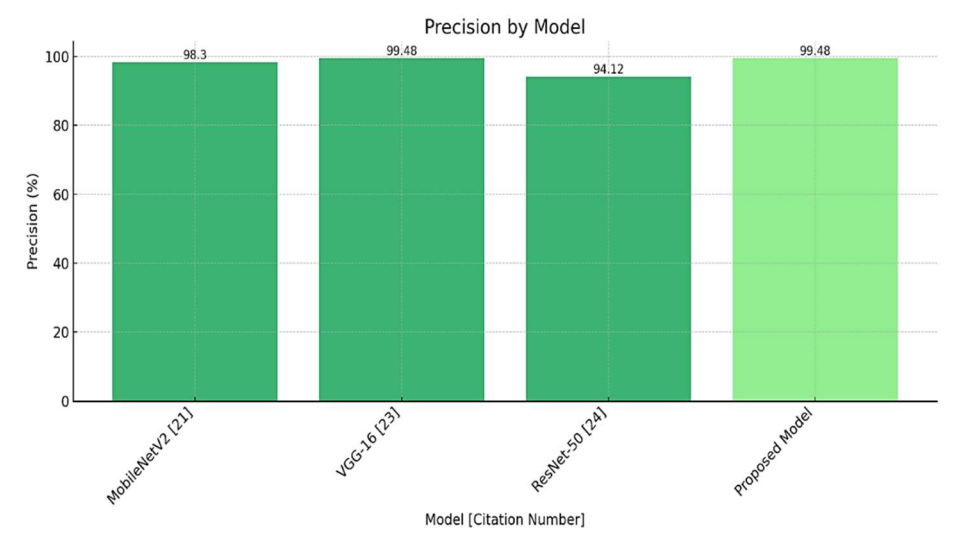


Figure 19: Precision Comparison Plot

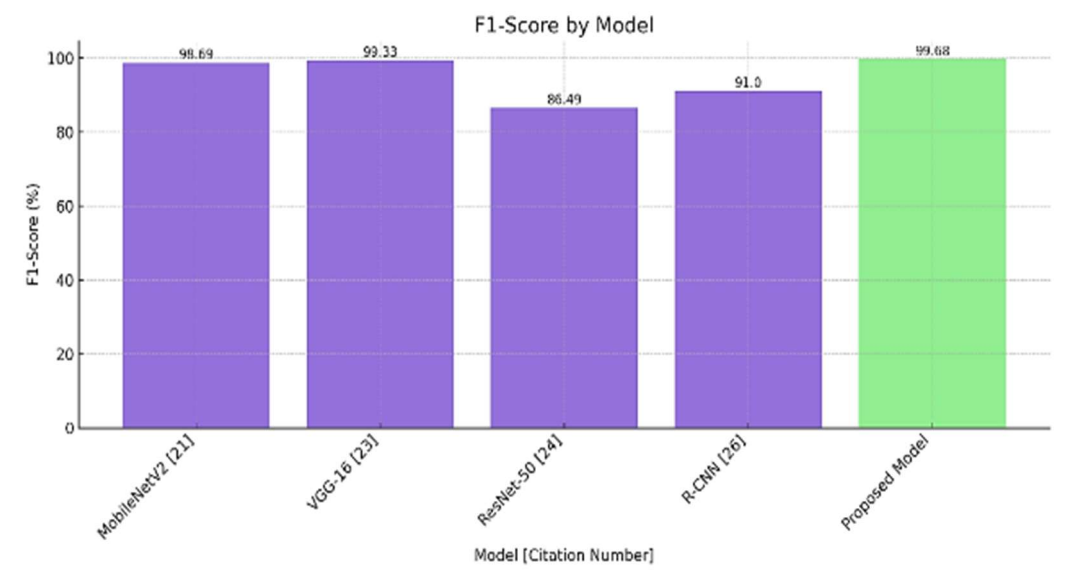


Figure 20: F1 Score Comparison plot

Table 8: F1-Score.

Model [Citation Number]	F1-Score (%)
MobileNetV2 [21]	98.69
VGG-16 with attention [23]	99.33
ResNet-50 [24]	86.49
R-CNN with Radiomics [26]	91
Proposed Model	99.68

The final table, Table 8, displays the F1-Score metrics. The proposed model achieves a score of 99.68%, which is higher than the scores of 99.33% achieved by VGG-16 with attention and 98.69% achieved by MobileNetV2. The F1-Score comparison plot that can be found in Figure 20

demonstrates that the model has a balanced performance in terms of precision and recall, which validates the model's overall effectiveness.

# 5. CONCLUSION

By combining the distinct capabilities of Inception V4, ResNet-50, and Bidirectional RNNs, IVRBR-Net represents a significant advancement in the field of breast cancer detection through thermographic imaging. The methodology incorporates rigorous preprocessing—including grayscale conversion, Multipurpose Beta Optimized Bi-histogram Equalization (MBOBHE), bilateral filtering, and the Affine Projection Algorithm (APA)—to enhance image quality. Feature extraction using Scale-

15<sup>th</sup> August 2025. Vol.103. No.15

© Little Lion Scientific



ISSN: 1992-8645 www.jatit.org E-ISSN: 1817-3195

Invariant Feature Transform (SIFT) and Haralick descriptors ensures that essential statistical properties are effectively captured, contributing to the model's exceptional performance. Tested on a dataset of 120 high-resolution thermographic images from the Database for Mastology Research (DMR), IVRBR-Net achieved remarkable metrics: accuracy of 99.82%, specificity of 99.74%, sensitivity of 99.35%, precision of 99.48%, and an F1-score of 99.68%. These results notably exceed those of state-of-the-art models current such as MobileNetV2, VGG-16 with attention, and ResNet-50, confirming IVRBR-Net's superior capability in accurate breast cancer detection. The integration of multi-scale feature extraction, deep residual learning, and bidirectional sequence analysis offers a dependable comprehensive and framework, enhancing early diagnosis and treatment planning, which can ultimately improve patient outcomes. However, while the study establishes a new benchmark in the field, several questions remain open for future exploration. For instance, how well does IVRBR-Net generalize to larger, more heterogeneous datasets collected from diverse populations and different imaging devices? The study does not address the model's robustness in real-world clinical settings where image quality and patient variability may be more pronounced. Additionally, the computational complexity and resource requirements of IVRBR-Net could pose challenges for deployment in low-resource or pointof-care environments-areas not explored in this work. Furthermore, while the model's accuracy is high, the interpretability of its predictions remains unexamined, raising important questions about explainability and clinician trust. Finally, the potential integration of multimodal data (such as combining thermography with ultrasound or MRI) to further enhance diagnostic accuracy is an avenue that this study does not pursue but could be valuable in future research. Addressing these questions will be crucial to translating the promising results of IVRBR-Net into practical clinical applications.

# ACKNOWLEDGEMENT

This work was carried out as part of a Post-Doctoral Research (Remote) at the Singapore Institute of Technology (SIT), Singapore. The author sincerely thanks to Dr. Tan Kuan Tak and Dr. Pravin Ramdas Kshirsagar for his continuous support and valuable suggestions, which greatly improved this work. The authors also acknowledge thanks to the Singapore Institute of Technology (SIT), Singapore for doing this Post-Doctoral Research (Remote).

#### **REFERENCES:**

- [1] A. Lashkari, F. Pak, and M. Firouzmand, "Full intelligent cancer classification of thermal breast images to assist physician in clinical diagnostic applications," *Journal of Medical Signals & Sensors*, Vol. 6, No. 1, 2016, p. 12.
- [2] A. Munguía-Siu, I. Vergara, and J. H. Espinoza-Rodríguez, "The use of hybrid CNN-RNN deep learning models to discriminate tumor tissue in dynamic breast thermography," Journal of Imaging, Vol. 10, No. 12, 2024, p. 329.
- [3] J. Selle, J. Josephine, A. Josephine Selle, B. Shenbagavalli, M. Venkatraman, M. Menaka, and M. Jayashree, "Automated Segmentation for Quantitative Analysis of Breast Thermograms." Proceedings of the 2015 Asia International Conference on Quantitative InfraRed Thermography, 2015.
- [4] Y. Zhou and C. Herman, "Optimization of skin cooling by computational modeling for early thermographic detection of breast cancer," *International Journal of Heat and Mass Transfer*, Vol. 126, 2018, pp. 864–876.
- [5] J. Koay, C. Herry and M. Frize, "Analysis of breast thermography with an artificial neural network," The 26th Annual International Conference of the IEEE Engineering in Medicine and Biology Society, San Francisco, CA, USA, 2004, pp. 1159-1162.
- [6] Globocan, "All Cancer. International Agency for Research on Cancer WHO (2019)", 2018. [Online]. Available: <a href="http://gco.iarc.fr/today/data/factsheets/cancers/3">http://gco.iarc.fr/today/data/factsheets/cancers/3</a> 9-All-cancers-fact-sheet.pdf.
- [7] M. Tahoun, A. A. Almazroi, M. A. Alqarni, T. Gaber, E. E. Mahmoud, and M. M. Eltoukhy, "A Grey Wolf-Based method for mammographic mass classification," *Applied Sciences*, Vol. 10, No. 23, 2020, p. 8422.
- [8] R. S. Patil and N. Biradar, "Automated mammogram breast cancer detection using the optimized combination of convolutional and recurrent neural network," *Evolutionary Intelligence*, Vol. 14, No. 4, 2020, pp. 1459– 1474.
- [9] H. Mousavi, and R. Bagherian, "Health literacy and breast cancer", *Health Psychology*, Vol. 8, No. 31, 2019, pp. 91-102.
- [10] A. Hossam, H. M. Harb, and H. M. A. E. Kader, "Automatic Image Segmentation Method For Breast Cancer Analysis Using Thermography," JES. Journal of Engineering Sciences/JES,

15th August 2025. Vol. 103. No. 15

© Little Lion Scientific



ISSN: 1992-8645 www.jatit.org E-ISSN: 1817-3195

- 2018, pp. 12–32.
- [11] U. R. Acharya, E. Y. K. Ng, J.-H. Tan, and S. V. Sree, "Thermography based breast cancer detection using texture features and support vector machine," Journal of Medical Systems, Vol. 36, No. 3, 2010, pp. 1503–1510.
- [12] S. S. Yadav and S. M. Jadhav, "Thermal infrared imaging based breast cancer diagnosis using machine learning techniques," Multimedia Tools and Applications, Vol. 81, No. 10, 2020, pp. 13139-13157.
- [13] E. A. Mohamed, E. A. Rashed, T. Gaber, and O. Karam, "Deep learning model for fully automated breast cancer detection system from thermograms," PLoS ONE, Vol. 17, No. 1, 2022, p. e0262349.
- [14] J. B. Awotunde, R. Panigrahi, B. Khandelwal, A. Garg, and A. K. Bhoi, "Breast cancer diagnosis based on hybrid rule-based feature selection with deep learning algorithm," Research Biomedical Engineering, Vol. 39, No. 1, 2023, pp. 115–127.
- [15] S. Yang, B. Deng, J. Wang, H. Li, M. Lu, Y. Che, X. Wei, and K. A. Loparo, "Scalable digital neuromorphic architecture for Large-Scale biophysically meaningful neural network with Multi-Compartment neurons," IEEE Transactions on Neural Networks and Learning Systems, Vol. 31, No. 1, 2019, pp. 148–162.
- [16] E. Y. K. Ng, U. Raghavendra, U. R. Acharya, J.-H. Tan, and A. Gudigar, "An Integrated Index for Breast Cancer Identification using Histogram of Oriented Gradient and Kernel Locality Preserving Projection Features Extracted from Thermograms," Proceedings of the 2010 International Conference on Quantitative *InfraRed Thermography*, 2016.
- [17] S. Ekici and H. Jawzal, "Breast cancer diagnosis using thermography and convolutional neural networks," Medical Hypotheses, Vol. 137, 2019, p. 109542.
- [18] "Banco de Imagens mastológicas." [Online]. Available: <a href="https://visual.ic.uff.br/dmi/">https://visual.ic.uff.br/dmi/</a>.
- [19][Online] Available: https://www.flir.in/browse/professionaltools/health-safety-amp-environmental/
- [20] S. Davies and J. Jacob, "Novel Algorithms for Early Cancer Diagnosis Using Transfer Learning with MobileNetV2 in Thermal Images," KSII Transactions on Internet and Information Systems, Vol. 18, No. 3, 2024.

- Journal of Engineering Sciences, Vol. 46, No. 1, [21] N. Berberian, H. Sargsyan, L. Sahakyan, A. G. Ghabuzyan, H. Geokchyan-Kzhdryan, S. Abnoosi, A. Leonian, K. D. Eriksson, and A. Gräwingholt, "Evaluation of an AI-powered portable thermal imaging solution as a prescreening tool for breast cancer," Cancer Screening and Prevention, Vol. 3, No. 1, 2024, pp. 8–15.
  - [22] A. Alshehri and D. AlSaeed, "Breast Cancer Diagnosis in Thermography Using Pre-Trained VGG16 with Deep Attention Mechanisms," Symmetry, Vol. 15, No. 3, 2023, p. 582.
  - [23] N. Aidossov, V. Zarikas, Y. Zhao, A. Mashekova, E. Y. K. Ng, O. Mukhmetov, Y. Mirasbekov, and A. Omirbayev, "An Integrated Intelligent System for Breast Cancer Detection at Early Stages Using IR Images and Machine Learning Methods with Explainability," SN Computer Science, Vol. 4, No. 2, 2023.
  - [24] S. U. R. Khan, A. Raza, N. M. T. Meeran, and U. Bilhaj, "Enhancing Breast Cancer Detection through Thermal Imaging and Customized 2D CNN Classifiers," VFAST Transactions on Software Engineering, Vol. 11, No. 4, 2023, pp. 80-92.
  - [25] M. P. L. Beuque, M. B. I. Lobbes, Y. Van Wijk, Y. Widaatalla, S. Primakov, M. Majer, C. Balleyguier, H. C. Woodruff, and P. Lambin, "Combining deep learning and handcrafted radiomics for classification of suspicious lesions mammograms," contrast-enhanced Radiology, Vol. 307, No. 5, 2023.
  - [26] S. Chatterjee, S. Biswas, A. Majee, S. Sen, D. Oliva, and R. Sarkar, "Breast cancer detection from thermal images using a Grunwald-Letnikov-aided Dragonfly algorithm-based deep feature selection method," Computers in Biology and Medicine, Vol. 141, 2021, p. 105027.
  - M. J. Mammoottil, L. J. Kulangara, A. S. Cherian, P. Mohandas, K. Hasikin, and M. Mahmud, "Detection of Breast Cancer from Five-View Thermal Images Using Convolutional Neural Networks," Journal of Healthcare Engineering, Vol. 2022, 2022, pp. 1-15.